

**PHOTOLUMINESCENT SIGNATURE OF ABSORBING MEDIUM WITH DEEP LEVELS BASED UPON
ABSORPTION COEFFICIENTS DERIVED FROM PARABOLIC-BAND APPROXIMATIONS**

Michael Y. Levy¹, N.J. Ekins-Daukes², Christiana Honsberg¹

¹Department of Electrical and Computer Engineering
University of Delaware
Newark, Delaware, USA 19716
mlevy@ece.gatech.edu, honsberg@ece.udel.edu

²School of Physics
University of Sydney,
Sydney, 2006 NSW, Australia
ned@physics.usyd.edu.au

ABSTRACT: This paper presents theoretical photoluminescent spectra of absorbing media each with valid quantum states forming an intermediate band. The novelty here is to illustrate the spectroscopic consequences of multi-gap absorbers whose quantum states form parabolic bands. Photoluminescence spectroscopy allows the band-edges of multiple transition solar cells to be investigated without additional complication of fabricating electrical contacts. Results are presented for absorbers with the same bandgaps, yet with distinct absorption characteristics, distinct temperatures, and distinct lengths. The authors draw two conclusions. First, the photoluminescent intensity of an intermediate band absorber may be appreciable within four distinct and well-separated spectral bands. Second, the full width at half maximum of the spectral band in the infrared regime approximates the width of the intermediate band.

Keywords: photoluminescence, fundamentals, intermediate band

1 INTRODUCTION

This paper presents theoretical photoluminescent spectra of absorbing media whose quantum states form a single intermediate band (IB). The work is relevant to several approaches that aim for high-efficiency solar energy conversion. These include multi-transition solar cells [1,2,3], and colloidal and epitaxial quantum dot solar cells [4], which may include multiple electron-hole pair generation [5]. Photoluminescence spectroscopy allows the band-edges of absorbers to be investigated. Therefore, properties of an absorber that are relevant to photovoltaic solar energy conversion may be examined without the additional complication of processing an absorbing medium into an actual solar cell [6,7]. Previous research examining the photoluminescent properties of absorbing media with an IB does so only for the most ideal of absorbing media [6,7].

The core novelty here is to illustrate the spectroscopic consequences of a multi-gap absorber whose energy-wavevector dispersion is given by parabolic bands [8, 9] (see Figure 1). In particular, the authors utilize absorption coefficients based on parabolic-band approximations to calculate the photon flows pumped into and sunk out of the IB absorber [10]. The authors stress that calculating the absorption coefficients under the parabolic-band approximations requires the absolute locations of three quasi-Fermi energies. This as opposed to calculations of the photon flows of IB absorbers based on idealized absorption coefficients [2,3,6,7,11,18] where only the three quasi-Fermi energy separations need be identified.

The remainder of this paper is organized as follows. In section two, the authors review relevant assumptions of the parabolic-band approximations. There, specific details of the absorption characteristics of the IB absorber are highlighted. Subsequently, in section three, the authors describe the procedure used to obtain the photoluminescent spectra. In section four, the authors offer the spectroscopic consequences of the parabolic bands. The results presented are largely invariant with respect to any particular absorption characteristics. In section five, the authors utilize the invariance of the

results to draw two conclusions.

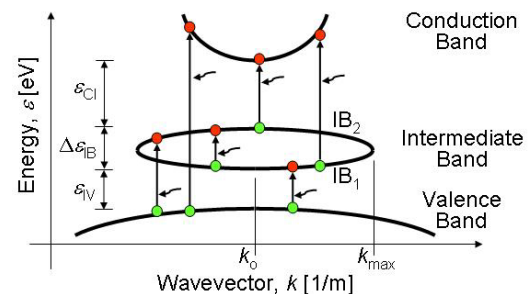


Figure 1: Energy-wavevector dispersion of a direct-gap intermediate-band absorbing medium under parabolic-band approximations. Photoluminescent spectra present here include contributions from six momentum-conserving photo-induced electronic transitions.

2 PARABOLIC-BAND APPROXIMATION

The PL spectra obtained here utilize absorption coefficients for an IB absorbing medium based on parabolic-band approximations, which are described in more detail in [8,9]. This section is divided in three parts. First, the authors review the major assumptions of the parabolic-band approximations. Second, the authors explain the phenomenon of parallel absorption paths and distinguish this from ideal spectral selectivity. Third, the authors clarify the consequences of k_{\max} and explain the role of k_{\max} in the subsequent presentation of data.

2.1 Parabolic-Band Assumptions

Figure 1 depicts the parabolic energy-wavevector dispersion that is here considered. The IB is comprised of two subbands (IB₁ and IB₂) and has a non-infinitesimal bandwidth, $\Delta\epsilon_{IB}$. The IB is separated from the conduction band (CB) and valence band (VB) by energetic gaps ϵ_{CI} and ϵ_{IV} , respectively. As shown, the model supposes a direct-gap medium so that the band extrema occur at the same wavevector, namely k_0 , which can for simplicity and without loss of generality assumed to be equal to zero. The parabolic-band approximation assumes that the quantum states in the IB must have a wavevector

between k_o and k_{max} (see Figure 1). Resulting from the parabolic-band approximations, six momentum-conserving photo-induced electronic transitions are permitted as shown in Figure 1.

2.2 Parallel Absorption Paths

Each of the momentum-conserving photo-induced electronic transitions has a quantifiable onset and offset of optical absorption, both of which depend on the difference between k_o and k_{max} [8,9]. The onset of absorption is that energy at which the absorption coefficient transitions from zero to a non-zero value and *vice versa* for the offset. A photon with an energy in the range $(\hbar\omega, \hbar\omega + d\hbar\omega)$ may induce any electronic transition whose onset of optical absorption is less than or equal to the photon's energy and whose offset of optical absorption is greater than the photon's energy. In other words, if in the range $(\hbar\omega, \hbar\omega + d\hbar\omega)$ the IB absorber's absorption characteristic has an absorption overlap [11], more than one parallel absorption paths are available to photons within this range. This contrasts with the notion of ideal spectral selectivity, whereby a photon definitively generates an electron-hole pair across the largest bandgap less than or equal to the photon's energy.

2.3 Role of Wavevector, k_{max}

The absorption characteristic of an IB absorbing medium that is yielded by the parabolic-band approximations is intimately related to the value of k_{max} of the IB absorbing medium. In the first place, k_{max} is related to the cube root of the concentration $[\#/m^3]$ of quantum states in the IB, which itself is linked to the absorption coefficients via the joint density of states [8]. In the second place, all else being equal save the effective masses of the intermediate band's subbands, the value of k_{max} may adjust the onsets and offsets of optical absorption [8,9].

As an example of the role of k_{max} , the authors now describe which of the absorption paths is most likely to convert a photon in the range $(1.40, 1.40 + d\hbar\omega)$ eV into an electron-hole pair. The energy range around 1.4 eV is of particular import as it is the threshold of the non-black emitter (see Figure 2) used to obtain the results present here. Based on the band parameters of the absorbers, which are roughly those given in Table III of reference [8,9]), when k_{max} is $1 \times 10^8 m^{-1}$, photons near 1.4 eV excite carriers from the VB to the CB. When k_{max} is $1 \times 10^9 m^{-1}$, there are three parallel absorption paths available to these photons; however, they will most likely excite carriers from the IB to the CB. When k_{max} is $3 \times 10^9 m^{-1}$, there are five parallel absorption paths available to these photons; however, these photons will primarily excite carriers from the VB to the IB.

Many of the major results given in this paper are given for distinct values of k_{max} (see Figure 3) or plotted with respect to k_{max} (see Figure 5). In either case, the authors utilize k_{max} to identify photoluminescent features that are entirely or largely invariant with respect to k_{max} , and hence invariant with respect to the particularities of the absorption characteristics. In this way, the authors identify features that have high likelihoods of being general photoluminescent properties of an IB absorbing medium as opposed to photoluminescent properties specific to a particular IB medium. Before offering the

major results, the authors first outline the necessary steps to calculate photoluminescent spectra. This is the topic of the following section.

3 SPECTROSCOPIC PROCEDURE

This section details the method used to obtain the photoluminescent spectra. First, the emission spectrum of a light emitting diode is chosen for the incident beam. Second, three (one each to describe the occupancy of the quantum states of each of the three electronic bands) quasi-Fermi levels are adjusted until two conditions are simultaneously obtained: (i) the carrier concentrations in the bands yield a charge neutral IB medium [8,9] and (ii) the net rate of electronic charge injected into each band of the IB medium is null. Upon converging to a solution, the emission spectrum [12] of the IB absorber is used to obtain its photoluminescent spectrum. These steps are now elucidated in more detail.

3.1 Incident Beam

The incident spectrum used to illuminate the samples is that emitted by a non-black emitter [13]. In determining the absorptivity of the non-black emitter, a null surface reflectivity is assumed and the absorption coefficients are calculated as for a semi-conductor [14]. Here, the length, temperature, and quasi-Fermi level separation of the non-black emitter are adjusted so that the photon flux [15] emitted is of the order of the solar irradiance at the Earth's surface concentrated 1000 times ($\sim 100 W/m^2$) and so that the full-width at half-maximum (FWHM) is 10 meV (see Figure 2). To generate this large photon flux, the non-black emitter is biased so that population inversion results. Here, the bandgap of the non-black emitter is set to 1.4 eV, which is greater than the largest bandgap of the IB absorbing media under test. It is assumed that the all of the photons emitted from the non-black emitter are incident upon the IB samples.

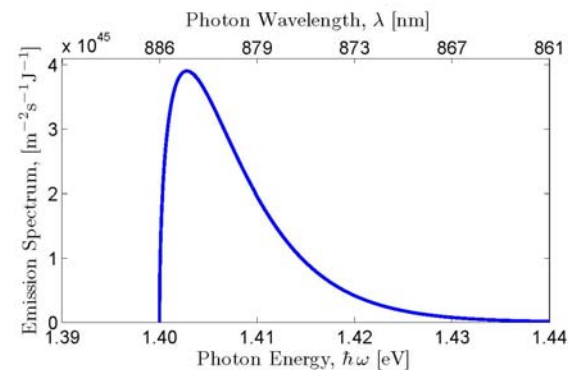


Figure 2: Simulated emission spectrum of the non-black emitter used to irradiate the intermediate band absorbers.

3.2 Net Charge Current

The net charge current injected into each band is calculated from the radiative flows and as in reference [10]. Here, it is assumed that only those photons emitted from the non-black emitter are incident upon the IB samples, that multiplicity [16] does not result from photon absorption, and that the net averaged non-radiative recombination rates are null. In calculating the photon flows pumped into and sunk out of each IB medium [10], the absorption coefficients resulting from parabolic approximation are employed [8,9]. These

absorption coefficients are used to calculate the absorptivity [12] of each IB sample. In so doing, surface reflectivity is assumed to be null.

3.3 Photoluminescent spectra

Upon converging to a simultaneous solution of the conditions stated in the introduction of this section, the photoluminescent spectra are obtained. The photoluminescent spectra for photons in the range $(\hbar\omega, \hbar\omega + d\hbar\omega)$ are given as the product of the photon energy, $\hbar\omega$, multiplied by the photon emission spectrum within this range [13]. The authors now proceed to give the results of the ongoing investigation.

4 INVARIANT PHOTOLUMINESCENT FEATURES

In this section, the authors illustrate and discuss two photoluminescent features that are invariant in the value of k_{max} . First, is the number of spectral bands that are present in the PL spectra. Second, is the FWHM of infrared component of the PL spectra. In obtaining the results presented here, the model parameters that are used are nearly those employed in reference [8,9].

4.1 Number of Spectral Bands

Figure 3 shows the photoluminescent spectra of three semi-infinite [17] IB absorbing media at 4 K. Each of these three samples have similar band structures, the only difference being that the effective masses of the intermediate band's subbands are adjusted to yield distinct values of k_{max} . Though there are differences in the exact appearance of PL spectra of each of these three absorbers, the authors concentrate attention on contrasting the gross characteristics of these spectra with PL spectra obtained from previous studies of the luminescent properties of such media [6,7].

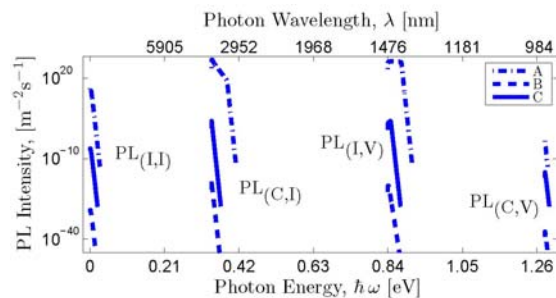


Figure 3: Photoluminescent spectra for three distinct semi-infinite [17] IB absorbing media at 4 K. Each absorber is distinct with respect to the maximum valid wavevector in the intermediate band: (A) $k_{max} = 1.1 \times 10^8 \text{ m}^{-1}$, (B) $k_{max} = 1.2 \times 10^9 \text{ m}^{-1}$ and (C) $k_{max} = 3.0 \times 10^9 \text{ m}^{-1}$. Please note that for visual clarity the magnitudes of plots B and C are scaled by 10^{-46} and 10^{-23} , respectively.

The first new characteristic is that each sample yields four, rather than three, spectral bands within which are contained a significant photoluminescent response. The leftmost spectral bands, $PL_{(I,I)}$, which are absent in references [6,7], result from momentum-conserving intraband photo-induced electronic processes between two distinct states in the IB. The remaining three peaks, $PL_{(C,I)}$, $PL_{(I,V)}$, and $PL_{(C,V)}$, result from photo-induced inter-band electronic processes between the CB and IB, the IB and VB, and the CB and VB, respectively. The onsets of all four spectral bands are identical to the onsets

of absorption defined in reference [8,9]. Similarly, the offset of the peak associated with intra-band processes is equal to the width of the IB [8,9].

The second new characteristic is that the apex of each luminescent peak in each spectral band does not, in general, occur at the optical absorption edge. Rather, the apexes occur at slightly larger energies. This results from the fact that under the parabolic-band approximations, the joint density of states at the absorption edges are null. Before moving on to the third major difference, the authors stress that the absorption edges of optical transitions are most fundamentally associated with the minimum energetic difference between any two distinct bands (see Figure 4). This is in contrast to a previous discussion of the absorption edges [18], where there the absorption edges are referenced to the quasi-Fermi level associated with the IB.

The third new characteristic is that the orders of magnitude of the apexes associated with the interband transitions at intermediate states are several orders of magnitude larger than those associated with the other electronic transitions. This results from the fact that the potential difference between the carriers in the CB and IB, $\epsilon_{F,CI}$, is near to if not greater than the onset optical absorption governing those photo-induced electronic transitions. A similar argument may be made regarding the potential difference between the carriers in the IB and VB, $\epsilon_{F,IV}$. Pane A of Figure 4 illustrates a case where there exists two distinct population inversions, which are illustrated by the negative absorptivity for photons in the ranges $(\epsilon_{CI}, \epsilon_{F,CI})$ and $(\epsilon_{IV}, \epsilon_{F,IV})$. Further, for photons within the range $(\epsilon_{CI}, \epsilon_{CI} + \Delta\hbar\omega)$ the absorptivity contains a sharp spike. The upshot is that extremely large emission results within these two spectral bands. Contrary to the results of pane A of Figure 4, the authors note that only a single range of negative absorptivity, namely between $(\epsilon_{CI}, \epsilon_{F,CI})$, is observed when parallel interband absorption paths exist for photons in the range $(\epsilon_{IV}, \epsilon_{F,IV})$.

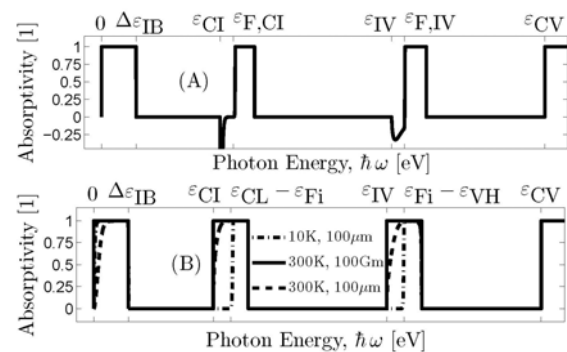


Figure 4: Absorptivity of IB absorbing media with k_{max} equal to $1.1 \times 10^8 \text{ m}^{-1}$. Pane (A) illustrates the non-equilibrium absorptivity of a semi-infinite medium at 4 K. Pane (B) illustrates the absorptivity of media with distinct lengths each of which is in equilibrium with a blackbody of the temperature listed.

The absorptivity given in pane A of Figure 4 may be compared with the three given in pane B of Figure 4. The absorptivity of each of the latter is obtained when the IB medium is in equilibrium with a blackbody. Note that at low temperature two of the optical edges appear shifted to higher energies. In particular, one edge appears at the

energetic difference between the CB edge, ε_{CL} , and the Fermi energy, ε_{Fi} ; while a second edge appears at the energetic difference between the Fermi energy and the VB edge, ε_{VH} . Though on close inspection, they are non-zero at the onsets given in Table I of reference [8,9].

In the following subsection, the authors make observations regarding the FWHM.

4.2 Full Width at Half Maximum

Figure 5 illustrates the FWHM of the spectral band associated with the photo-induced electronic transitions between two distinct states of the IB. Shown are nine curves plotted with respect to k_{max} . Each of the curves is associated with an absorber whose temperature and length are distinct from all the others. It is clear that the FWHM increases with increasing temperature. At temperatures near absolute zero the FWHM range between 1 meV and 4 meV, which are less than the FWHM of the incident beam. Finally, at room temperature the FWHM range between 50 meV and 80 meV, which are less than the widths of the IB considered here (*i.e.* here, as in reference [8,9], the widths of the IB are uniformly 100 meV). The following section provides concluding remarks.

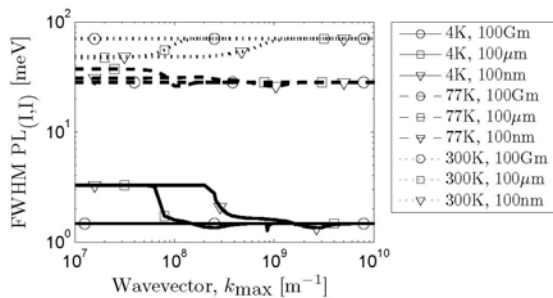


Figure 5: The full width at half maximum (FWHM) of the spectral band associated with intraband electronic transitions between distinct states of the intermediate band (*i.e.* $PL_{(L)}$). Each of the nice plots is associated with an absorber whose temperature and length are distinct from all the others (see legend).

5 CONCLUSIONS

This paper illustrates the spectral consequences of intermediate band absorbers under parabolic-band approximations. The results present here are obtained for absorbers with similar band structures. However, the absorbers are distinct with respect to their temperatures, their lengths, and their absorption characteristics. By directing attention to those results that are largely or completely invariant with respect to the nuances of the absorption characteristics, the authors are able to draw strong conclusions. The authors draw two conclusions regarding the photoluminescent spectra of an absorber with quantum states forming a band of a non-infinitesimal width that is electronically isolated from both the conduction and valence bands and that has a bandwidth smaller than the smallest bandgap in the absorber. First, the resulting PL spectra will have content within four well-separated spectral bands. Second, the full-width at half-maximum of the spectral band in the infrared regime is less than the energetic bandwidth of the quantum states forming the intermediate band. This is important as it allows an empirical measure of the energetic width of the deep quantum states.

ACKNOWLEDGEMENTS

M.Y.L. and C.H. give thanks to the U.S. National Renewable Energy Laboratory for their financial support through subcontract XAT-5-44277-01 administered by M. Symko-Davies and R. McConnell.

- [1] M. Wolf, Proceedings of the Institute of Radio Engineers, Vol. 48 (1960) 1246.
- [2] A. Luque, A. Martí, Physical Review Letters 78 (1997) 5014.
- [3] A.S. Brown, M.A. Green, R.P. Corkish, Physica E 14 (2002) 121.
- [4] A.J. Nozik, Physica E 14 (2002) 115.
- [5] R.D. Shaller, V.I. Klimov, Physical Review Letters 92 (2004) 186601.
- [6] N.J. Ekins-Daukes, C. Honsberg, M.Y. Levy, M. Yamaguchi, in process for submission to Physical Review B (2007).
- [7] N.J. Ekins-Daukes, C. Honsberg, M. Yamaguchi, Proceedings of the Thirty-First IEEE Photovoltaic Specialist Conference 31 (2005) 49.
- [8] M.Y. Levy, C. Honsberg, "Modeling of Nanostructured Materials; Photo-absorption based on Parabolic Band Approximations," National Renewable Energy Laboratory Technical Report for Contract XAT-5-44277-01 (Aug. 3, 2007)
- [9] M.Y. Levy, C. Honsberg, Physical Review B, in process for submission (2007).
- [10] M.Y. Levy, C. Honsberg, IEEE Electron Device Letters, in process for submission (2007).
- [11] L. Cuadra, A. Martí, A. Luque, IEEE Transactions on Electron Devices 51 (2007) 1002.
- [12] M.Y. Levy, C. Honsberg, Proceedings of 4th World Conference on Photovoltaic Energy Conversion, (2006) 71.
- [13] P. Würfel, Journal of Physics C 15 (1982) 3967.
- [14] E. Rosencher, B. Vinter, Optoelectronics, Cambridge University Press (2002) 304.
- [15] A. De Vos, Endoreversible Thermodynamics of Solar Energy Conversion, Oxford University Press (1992) 11.
- [16] A. De Vos, B. Desoete, Solar Energy Materials and Solar Cells 51 (1998) 413.
- [17] The absorptivity of a semi-infinite medium will exhibit very sharp transitions (see Figure 4). In addition, a semi-infinite medium will push the computer towards its numerical tolerance. Here, calculations that refer to a semi-infinite are equivalent to a length of 100 gigameters.
- [18] A. Luque, A. Martí, Progress in Photovoltaic 9 (2001) 73.